Data Repository Item

U-Pb Analytical Methods

Zircons were separated from each of the seven 1 to 4 kg samples samples (see Fig. 1 for locations) by standard crushing and gravimetric techniques, picked in alcohol on the basis of lack of inclusions and fractures, mounted in 2.54 cm epoxy rounds, and polished to expose the grain interiors. Cathodoluminesence (CL) and transmitted/reflected light images were used to characterize the grains and select spots for analysis. Zircons were analyzed for U-Pb on the SHRIMP-RG (sensitive high resolution ion microprobe-reverse geometry) instrument at the United States Geological Survey-Stanford University Ion Probe Laboratory, Stanford, CA. A spot size of ca. 25-30 µm in diameter was used for all analyses. The analytical routine followed Williams (1998) and Barth et al. (2001) and data reduction and age calculation utilized the SQUID program of Ludwig (2001). The concentration of U was calibrated using zircon standard CZ3 (U = 550 ppm). Isotopic compositions were calibrated by replicate analyses of zircon standard R33 (419 Ma; Black et al., 2004). Zircons from the samples were analyzed over several sessions and several different mounts. Calibration errors for the $^{206}Pb/^{238}U$ ratios of R33 for the three different analytical sessions were 0.55%, 0.87%, and 0.38% (2σ). Discussion and interpretation of analyses are based on the weighted mean of $^{206}Pb/^{238}U$ ages calculated from ratios corrected for common Pb using the ^{207}Pb method. Common Pb compositions were estimated from Stacey and Kramers (1975). Analyses were grouped by age and interpreted in context of core versus rim domains determined by CL imaging and allowance for isotopic complexity due to the effects of inheritance, Pb-loss, or metamorphic overgrowths. Ages were calculated as inverse-variance weighted mean $^{206}Pb/^{238}U$ ages with errors reported at the 95% confidence level. Tera-Wasserburg diagrams were generated with the Isoplot/Ex program of Ludwig (2003). Analytical results are presented in Table DR1 and plotted in Figure DR2.

Data Repository Item

Figure DR1. Lower-hemisphere, equal-area projections of structural fabric data from four study areas in the transition between the western Idaho shear zone and Orofino shear zone in west-central Idaho (see Fig. 1 for locations). Five generations of superposed structures are recognized in the region. First structures (D1) consist of at least two generations of nearly parallel penetrative foliations and folds. D2 and D3 structures consist of folds, cleavage, and mylonitic fabrics that are related to the western Idaho shear zone and Orofino shear zone, respectively. D4 and D5 structures are minor folds and crenulation cleavage associated with low-strain deformation that post-dates the Orofino shear zone. Along the South Fork of the Clearwater River, superposition relations between pre-145 Ma structures in rocks of the Salmon River belt (D1) and younger northeast-trending foliations (D2) of the western Idaho shear zone are well established. Along the Middle Fork of the Clearwater River, D1 structures are found in rocks of the Salmon River belt and in schist and gneiss with Proterozoic and Mesozoic protoliths and are overprinted by northeast-trending foliations (D2) of the western Idaho shear zone. From the South Fork to the Middle Fork, northwest-trending minor folds with crenulation and spaced cleavage (D3) attributed to the Orofino shear zone progressively increase in development from south to north. At Greer, a Jura-Cretaceous quartz diorite plutonic complex (Kauffman et al., 2006) is deformed in western Idaho shear zone structures (D2) that consist of at least two penetrative foliations that are progressively transposed into near parallelism with D3 mylonitic fabrics of the Orofino shear zone. At Dworshak, parageneiss contains D1 structures that consist of at least two generations of nearly parallel isoclinal folds with a pervasive penetrative axial-planar cleavage; the folds are defined by compositional layering in meta-sedimentary rocks assigned to the Salmon River belt. The composite D1 structures at Dworshak are interpreted to be transposed equivalents of the Salmon River belt and possibly of the western Idaho shear zone to the south. At Greer, early structures (D2) are, from south to north over a distance of a few hundred meters, progressively transposed into the fabrics of the Orofino shear zone where D3 structures consist of SC mylonite with top-to-the south shear indicated by tails on feldspar porphyblasts. The strain increases from the margin to the interior of the shear zone and is reflected in the progressive decrease in SC angle to essentially zero and an associated increase in foliation dip from ~30° to ~80° over distances of a few hundred meters. The D3 mylonite is divided into at least two generations with steeply dipping structures over-printed by shallowly north-dipping SC mylonite. At Dworshak, S and C surfaces of D3 structures are essentially parallel and represent the first generation of fabric within the Cretaceous tonalite (~90 to ~70 Ma) contained within the Orofino shear zone.

Data Repository Item

TABLE DR1. U-Pb SHRIMP GEOCHRONOLOGIC DATA AND APPARENT AGES

Spot	U† (ppm)	Th (ppm)	Th/U	^{206}Pb*† (ppm)	f^{206}Pb$_c$†	^{238}U/^{206}Pb§		^{207}Pb/^{206}Pb§		^{206}Pb/^{238}U# (Ma)	
Sample 1. Trondhjemite (99-01) (N 45° 54' 30.9"; W 116° 00' 28.5")											
1.1	170	18	0.1	2	1.9	59.47	(4)	0.0629	(13)	106	(4)
2.1	234	37	0.2	3	0.5	57.95	(3)	0.0525	(11)	110	(3)
3.1	211	36	0.2	3	0.3	58.52	(3)	0.0505	(11)	109	(3)
4.1	180	29	0.2	3	-	56.35	(4)	0.0469	(12)	114	(4)
5.1	499	73	0.2	8	0.4	56.46	(2)	0.0517	(7)	113	(2)
6.1	327	63	0.2	5	1.8	58.56	(3)	0.0622	(8)	107	(3)
7.1	271	47	0.2	4	1.0	56.15	(3)	0.0560	(10)	113	(3)
7.2	179	32	0.2	3	3.6	56.68	(4)	0.0765	(17)	109	(5)
8.1	245	38	0.2	4	1.0	56.85	(3)	0.0559	(10)	111	(3)
9.1	206	46	0.2	3	0.6	57.53	(3)	0.0530	(11)	110	(4)
10.1	404	64	0.2	6	0.5	56.91	(2)	0.0523	(8)	112	(3)
11.1	225	44	0.2	4	-	53.95	(3)	0.0473	(11)	119	(4)
12.1	327	62	0.2	5	0.0	57.23	(3)	0.0480	(12)	112	(3)
13.1	414	91	0.2	6	0.3	58.31	(2)	0.0503	(8)	109	(2)
14.1	92	8	0.1	1	1.9	57.37	(5)	0.0629	(16)	109	(6)
Sample 2. Biotite tonalite (99-02) (N 45° 49' 26.4"; W 115° 54' 55.8")											
1.1	564	257	0.5	6	-	77.49	(2)	0.0466	(2)	83	(2)
2.1	218	110	0.5	2	2.1	77.87	(4)	0.0647	(4)	81	(3)
3.1	105	75	0.7	1	0.7	66.59	(5)	0.0532	(5)	95	(5)
4.1	752	274	0.4	8	0.4	76.79	(2)	0.0507	(2)	83	(2)
5.1	641	222	0.4	8	0.1	72.83	(2)	0.0489	(2)	88	(2)
6.1	686	387	0.6	9	-	67.70	(2)	0.0460	(2)	95	(2)
7.1	522	218	0.4	6	1.7	72.00	(2)	0.0610	(2)	87	(2)
8.1	565	208	0.4	7	0.1	72.62	(2)	0.0485	(2)	88	(2)
9.1	377	154	0.4	5	0.5	67.21	(3)	0.0519	(3)	95	(3)
9.2	517	220	0.4	7	0.2	66.14	(2)	0.0497	(2)	97	(2)
10.1	119	15	0.1	1	-	74.92	(5)	0.0431	(5)	86	(4)
11.1	505	188	0.4	6	0.1	76.50	(2)	0.0483	(2)	84	(2)
12.1	397	170	0.4	4	0.9	76.94	(3)	0.0551	(3)	82	(2)
12.2	389	125	0.3	5	0.1	72.46	(3)	0.0490	(3)	88	(2)
13.1	540	183	0.3	6	0.4	75.60	(2)	0.0508	(2)	84	(2)
14.1	514	197	0.4	6	1	72.36	(2)	0.0546	(2)	88	(2)
Sample 3. Biotite tonalite (00-84) (N 46° 31' 42.5"; W 116° 17' 27.4")											
1.1	97	17	0.2	3	0.7	28.21	(2)	0.0559	(5)	223	(4)
2.1	253	13	0.1	3	0.6	72.53	(2)	0.0522	(6)	88	(1)
3.1	171	49	0.3	6	0.2	26.47	(1)	0.0525	(4)	239	(3)
4.1	1547	2	0.001	20	0.2	67.25	(1)	0.0498	(2)	95	(1)
5.1	824	12	0.015	10	0.8	73.04	(1)	0.0544	(3)	87	(1)
6.1	168	46	0.3	5	0.4	26.55	(1)	0.0540	(4)	237	(3)
7.1	41	9	0.2	1	8.3	36.72	(3)	0.1151	(11)	159	(5)

Spot	U† (ppm)	Th (ppm)	Th/U	$^{206}Pb^{*\dagger}$ (ppm)	$f^{206}Pb_c{}^{\dagger}$	$^{238}U/^{206}Pb^{\S}$		$^{207}Pb/^{206}Pb^{\S}$		$^{206}Pb/^{238}U^{\#}$ (Ma)	
Sample 3 (CONTINUED)											
8.1	1019	156	0.2	21	-	41.97	(0.6)	0.0484	(2)	152	(1)
9.1	2921	6	0.002	36	0.2	69.87	(0.4)	0.0497	(2)	91	(0)
10.1	1096	2	0.002	13	0.2	71.39	(0.7)	0.0491	(3)	90	(1)
11.1	1630	518	0.3	51	0.2	27.32	(0.4)	0.0525	(1)	231	(1)
12.1	1522	359	0.2	49	0.0	26.82	(0.5)	0.0506	(2)	236	(1)
13.1	2224	450	0.2	71	0.1	26.80	(0.4)	0.0516	(1)	236	(1)
14.1	1425	157	0.1	39	0.1	31.76	(0.5)	0.0507	(2)	200	(1)
Sample 4. Hornblende-biotite quartz diorite (00-86) (N 46° 33’ 25.3”; W 116° 16’ 0.3”)											
1.1	360	129	0.4	4	-	72.77	(1.7)	0.0456	(7)	88	(2)
2.1	467	163	0.4	6	0.4	72.18	(1.5)	0.0508	(6)	88	(1)
3.1	802	122	0.2	9	-	75.77	(1.2)	0.0466	(5)	85	(1)
4.1	443	185	0.4	5	-	70.44	(1.6)	0.0455	(6)	91	(1)
5.1	640	173	0.3	8	-	71.99	(1.4)	0.0472	(5)	89	(1)
5.2	476	170	0.4	6	0.5	67.00	(1.9)	0.0517	(7)	95	(2)
6.1	446	181	0.4	5	0.2	72.23	(1.6)	0.0498	(6)	88	(1)
7.1	369	158	0.4	4	0.1	71.93	(1.7)	0.0490	(7)	89	(2)
8.1	611	177	0.3	7	0.1	71.11	(1.3)	0.0484	(5)	90	(1)
9.1	398	185	0.5	5	0.6	70.86	(1.8)	0.0529	(7)	90	(2)
10.1	337	165	0.5	4	-	70.52	(1.8)	0.0475	(7)	91	(2)
11.1	208	174	0.9	56	1.2	3.19	(0.7)	0.1169	(2)	1739	(13)
12.1	142	109	0.8	2	-	74.13	(3.0)	0.0449	(12)	87	(3)
13.1	464	147	0.3	5	0.0	72.88	(1.4)	0.0479	(6)	88	(1)
14.1	587	136	0.2	7	-	71.73	(1.4)	0.0449	(6)	90	(1)
15.1	722	163	0.2	9	0.4	70.68	(1.2)	0.0510	(5)	90	(1)
Sample 5. Hornblende-biotite tonalite (01JPA) (N 46 18’ 37.6”; W 115 48’ 05.9”)											
1.1	486	209	0.4	5	0.9	86.60	(2.1)	0.0543	(9)	73	(2)
2.1	251	88	0.4	2	-	89.39	(2.9)	0.0463	(11)	72	(2)
3.1	200	63	0.3	2	4.8	88.34	(3.8)	0.0858	(11)	69	(3)
4.1	328	203	0.6	3	0.4	87.87	(3.0)	0.0509	(13)	73	(2)
5.1	205	93	0.5	2	-	86.76	(3.4)	0.0469	(16)	74	(3)
6.1	338	208	0.6	3	0.5	89.47	(4.5)	0.0515	(10)	71	(3)
7.1	372	157	0.4	4	-	88.75	(2.8)	0.0426	(11)	73	(2)
8.1	267	108	0.4	3	1.1	82.08	(3.3)	0.0564	(11)	77	(3)
9.1	292	121	0.4	3	-	85.85	(3.3)	0.0439	(13)	75	(3)
10.1	305	135	0.5	3	0.1	91.26	(3.4)	0.0483	(17)	70	(2)
11.1	375	160	0.4	4	1.0	84.21	(2.8)	0.0554	(10)	75	(2)
12.1	191	63	0.3	2	0.7	99.46	(4.2)	0.0532	(15)	64	(3)
13.1	287	112	0.4	3	-	83.13	(3.2)	0.0469	(12)	77	(2)
14.1	366	147	0.4	4	-	87.40	(2.9)	0.0462	(11)	73	(2)

Data Repository Item

Spot	U[†] (ppm)	Th (ppm)	Th/U	$^{206}Pb^{*\dagger}$ (ppm)	$f^{206}Pb_c^{\dagger}$	$^{238}U/^{206}Pb^{\S}$		$^{207}Pb/^{206}Pb^{\S}$		$^{206}Pb/^{238}U^{\#}$ (Ma)	
Sample 6. Leucocratic pegmatite (01JPC) (N 46 30' 42.7"; W 116 19' 35.9")											
1.1	557	26	0.05	6	-	74.77	(1.9)	0.0397	(7)	87	(2)
2.1	278	10	0.04	3	-	74.94	(2.6)	0.0365	(11)	87	(2)
3.1	66	26	0.4	1	-	62.34	(7.2)	0.0403	(16)	104	(8)
4.1	379	23	0.06	5	0.8	72.28	(2.1)	0.0539	(7)	88	(2)
5.1	79	21	0.3	1	0.4	71.63	(4.8)	0.0508	(17)	89	(4)
6.1	533	26	0.05	6	-	72.56	(1.9)	0.0454	(7)	89	(2)
7.1	134	40	0.3	2	1.2	70.80	(3.6)	0.0573	(14)	89	(3)
8.1	566	28	0.05	6	0.7	76.98	(1.9)	0.0532	(6)	83	(2)
9.1	188	70	0.4	2	0.1	72.32	(4.6)	0.0489	(12)	88	(4)
Sample 7. Leucocratic pegmatite (01JPB) (N 46 18' 38.4"; W 115 48' 04.7")											
1.1	209	99	0.5	2	1.1	83.36	(3.7)	0.0563	(13)	76	(3)
2.1	138	42	0.3	1	-	86.90	(4.6)	0.0433	(18)	74	(3)
3.1	189	53	0.3	2	-	94.32	(3.9)	0.0404	(16)	69	(3)
4.1	220	93	0.4	2	-	86.59	(3.5)	0.0427	(14)	74	(3)
5.1	470	462	1.0	5	-	85.99	(2.4)	0.0424	(12)	75	(2)
6.1	194	100	0.5	2	1.6	93.95	(3.9)	0.0598	(14)	67	(3)
7.1	224	111	0.5	3	0.0	73.51	(4.0)	0.0481	(13)	87	(4)
8.1	229	116	0.5	2	0.0	85.95	(3.7)	0.0474	(14)	75	(3)
9.1	363	156	0.4	4	0.9	87.39	(3.0)	0.0545	(10)	73	(2)
9.2	348	278	0.8	71	0.8	4.21	(0.9)	0.0943	(2)	1364	(12)
10.1	55	49	0.9	0.5	2.6	95.25	(7.5)	0.0676	(24)	66	(5)
11.1	392	159	0.4	4	-	86.81	(2.8)	0.0463	(11)	74	(2)
11.2	419	173	0.4	4	0.7	85.07	(2.3)	0.0533	(8)	75	(2)
12.1	376	166	0.5	4	0.2	89.37	(2.8)	0.0489	(10)	72	(2)
12.2	389	257	0.7	4	0.1	89.06	(2.5)	0.0485	(10)	72	(2)
13.1	290	120	0.4	3	2.1	97.04	(3.5)	0.0639	(10)	65	(2)
14.1	401	283	0.7	4	0.6	89.74	(2.7)	0.0525	(9)	71	(2)
15.1	186	62	0.3	2	-	89.64	(3.9)	0.0440	(14)	72	(3)
16.1	288	174	0.6	3	0.5	83.84	(3.0)	0.0513	(19)	76	(2)
17.1	365	144	0.4	4	-	87.69	(2.9)	0.0461	(17)	73	(2)
18.1	269	101	0.4	3	0.4	89.11	(2.9)	0.0504	(10)	72	(2)
18.2	197	79	0.4	2	-	87.34	(3.4)	0.0427	(13)	74	(3)

Note: All analyses were performed on the SHRIMP-RG (sensitive high mass resolution ion microprobe - reverse geometry) ion microprobe at the United States Geological Survey-Stanford Microanalytical Center, Stanford, CA.

† Pb* denotes radiogenic Pb; Pb_c denotes common Pb; $f^{206}Pb_c = 100*(^{206}Pb_c/^{206}Pb_{total})$.

§ Reported ratios are not corrected for common Pb. Errors are reported in parentheses as percent at the 1 σ level.

\# Ages calculated from ratios corrected for common Pb using ^{207}Pb for the $^{206}Pb/^{238}U$ age. Uncertainties in millions of years reported as 1 σ.

References

Barth, A.P., Wooden, J.L. & Coleman, D.S., 2001, SHRIMP-RG U-Pb zircon geochronology of Mesoproterozoic metamorphism and plutonism in the southwesternmost United States: Journal of Geology, v. 109, p. 319-327.

Black, L.P., Kamo, S.L., Allen, C.M., Davis, D.W., Aleinikoff, J.N., Valley, J.W., Mundil, R., Campbell, I.H., Korsch, R.J., Williams, I.S., and Foudoulis, C., 2004, Improved $^{206}Pb/^{238}U$ microprobe geochronology by the monitoring of a trace-element related matrix effect; SHRIMP, ID-TIMS, ELA-ICP-MS and oxygen isotope documentation for a series of zircon standards: Chemical Geology, v. 205, p. 115–140.

Kauffman, J.D., Garwood, D.L., Schmidt, K.L., Lewis, R.S., Othberg, K.L., and Phillips, W.M., 2006, Geologic map of the Idaho parts of the Orofino and Clarkston 30 x 60 minute quadrangles: Idaho Geological Survey Digital Map Map 69, scale 1:100,000.

Ludwig, K.R., 2001, Squid version 1.02: A users manual. Berkeley Geochronology Center Special Publication 1, p. 1-22.

Ludwig, K.R., 2003, User's manual for Isoplot 3.00: a geochronological toolkit for Microsoft Excel: Berkeley Geochronology Center Special Publication 4, p. 1-70.

Stacey J.S., and Kramers, J.D., 1975, Approximation of terrestrial lead isotope evolution by a two-stage model: Earth and Planetary Science Letters, v. 26, p. 207-221.

Williams, I.S., 1998, U-Pb by ion microprobe, *in* McKibben, M.A., Shanks, W.C., and Ridley, W.I., eds., Applications of microanalytical techniques to understanding mineralizing processes: Society of Economic Geologists, Reviews in Economic Geology 7, p. 1-35.

Data Repository Item

DR2007185

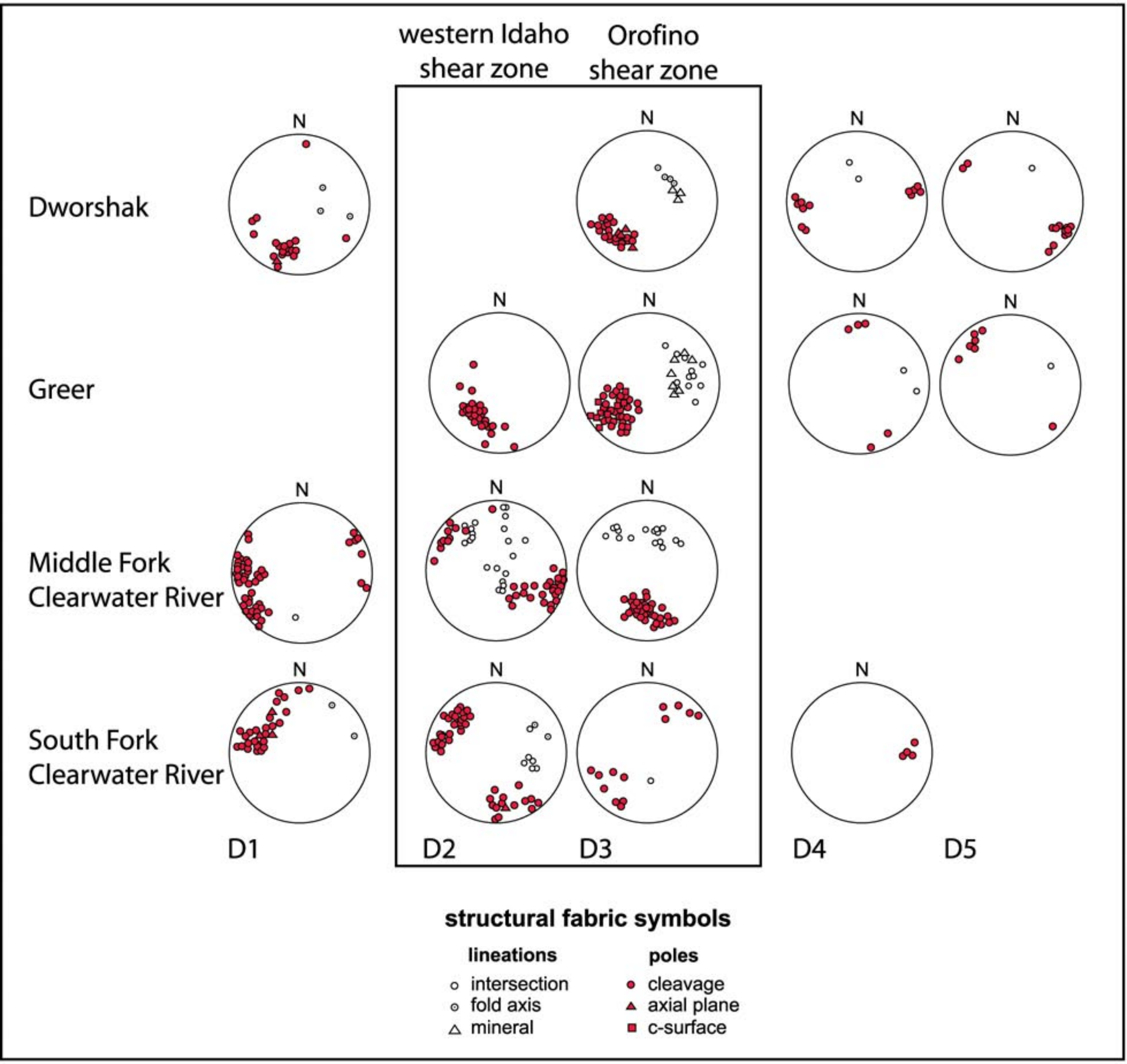

Figure DR1. See figure caption on following page for explanation.

Data Repository Item

DR2007185

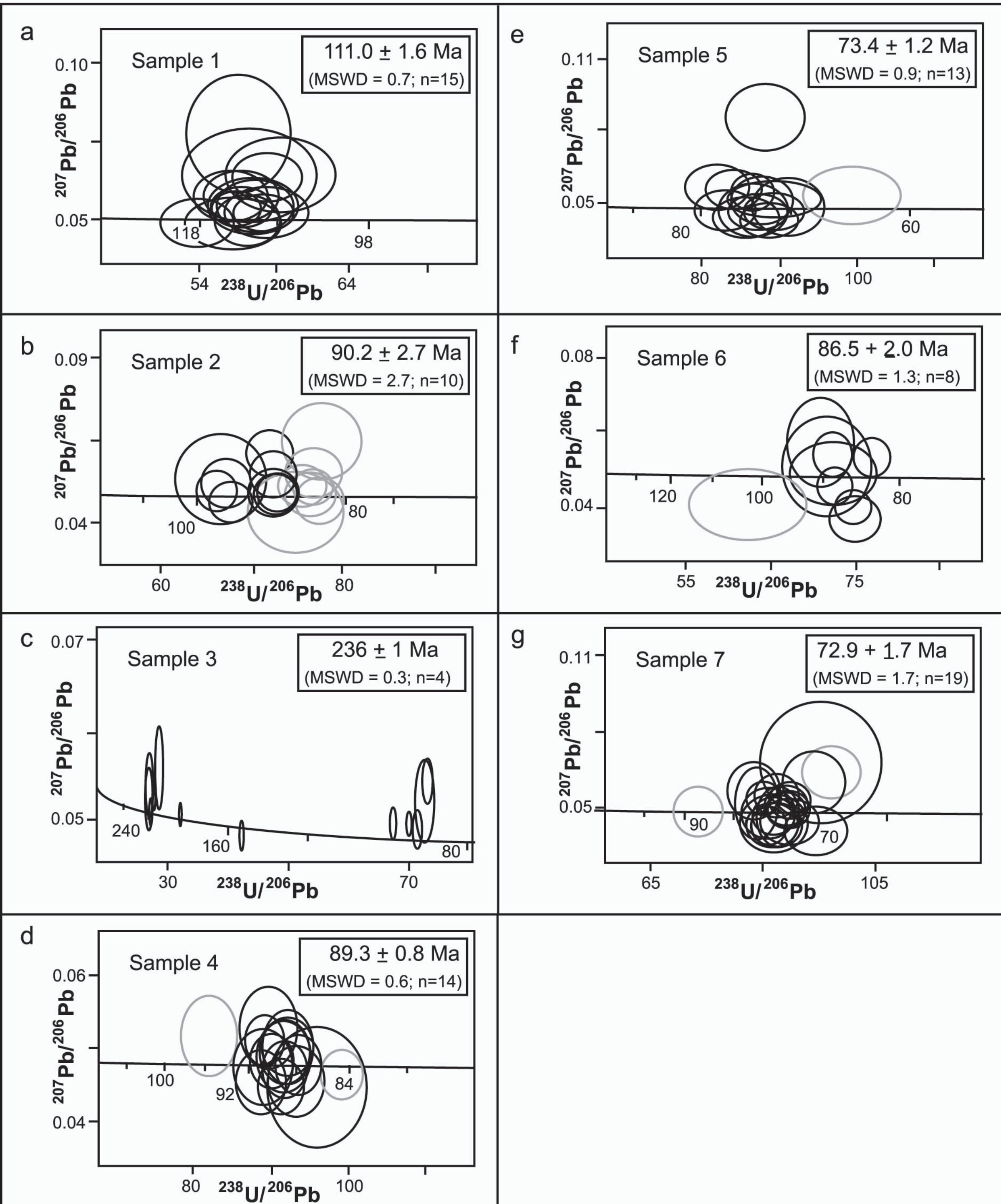

Figure DR2. Tera-Wasserburg plots of SHRIMP-RG U-Pb zircon data from sampled units (see Fig.1 for locations). Data are plotted uncorrected for common Pb as 1σ error ellipses. Black ellipses were used in calculation of weighted mean $^{206}Pb/^{238}U$ ages cited with errors at 95% confidence level. Grey ellipses were excluded assuming that excess scatter in $^{206}Pb/^{238}U$ ages reflects inheritance, Pb-loss, or metamorphic overgrowth.